Cell Proliferation

Cell Prolif., 2011, **44**, 183–191 doi: 10.1111/j.1365-2184.2011.00737.x

Immobilization of thrombocytes on PCL nanofibres enhances chondrocyte proliferation *in vitro*

R. Jakubova*,†, A. Mickova*,†, M. Buzgo*,§, M. Rampichova†, E. Prosecka*,†, D. Tvrdik‡ and E. Amler*,†

**Institute of Biophysics, 2nd Faculty of Medicine, Charles University in Prague, Prague, Czech Republic, †Laboratory of Tissue Engineering, Institute of Experimental Medicine, Academy of Sciences of the Czech Republic, Prague, Czech Republic, ‡Institute of Pathology, First Faculty of Medicine and General Teaching Hospital, Charles University, Prague, Czech Republic, and §Department of Cell Biology, Faculty of Science, Charles University in Prague, Prague, Czech Republic*

Received 16 *July* 2010; *revision accepted* 10 *October* 2010

Abstract

Objectives: The aim of this study was to develop functionalized nanofibres as a simple delivery system for growth factors (GFs) and make nanofibre cell-seeded scaffold implants a one-step intervention.

Materials and methods: We have functionalized polycaprolactone (PCL) nanofibres with thrombocytes adherent on them. Immobilized, these thrombocytes attached to nanofibre scaffolds were used as a nanoscale delivery system for native (autologous) proliferation and differentiation factors, *in vitro*. Pig chondrocytes were seeded on the thrombocyte-coated scaffolds and levels of proliferation and differentiation of these cells were compared with those seeded on non-coated scaffolds.

Results: Immobilized thrombocytes on PCL nanofibres effectively enhanced chondrocyte proliferation due to time-dependent degradation of thrombocytes and release of their GFs.

Conclusions: These simply functionalized scaffolds present new possibilities for nanofibre applications, as smart cell scaffolds equipped with a GF delivery tool.

Introduction

Blood flow is pivotal to regeneration of connective tissues. The positive role of blood reparative cells (1,2) as well as blood derivatives (3) in the healing process has previously been clearly proven. In addition, pluripotent mesenchymal stem cells (MSC) are known to differentiate into connective tissue cells and have been found in bone marrow and blood (4). Circulation-derived cells also temporarily present in a wounded area in early phases of the healing process of tendons (5). Moreover, the principal phagocytic cells in healing wounds are also of blood origin (6). These findings suggest that locally injected blood derivatives could be useful as activators of circulation-derived cells for initial enhancement of healing.

Platelet-rich plasma (PRP) is a blood derivative of platelets in a small volume of plasma. Its role in regeneration of bone (7–9), cartilage (10,11) and ligaments (12) has been recently investigated. PRP is known to contain several GFs including platelet-derived growth factor, transforming growth factor β, fibroblastic growth factor, vascular endothelial growth factor, insulin-like growth factor-1 and epidermal growth factor (13,14). Consequently, PRP applications in tissue engineering seem highly promising to clinicians and researchers. Delocalization and volatility however, remain among the main constraints to broader application of PRP. To keep concentrations at bioactive levels needed for healing, an appropriate system for their immobilization must be developed. Naturally, this system should be biocompatible and preferably biodegradable.

Nanofibres have recently been used in tissue engineering (7). Their greatest asset is that their size and shape can match those of cells and extracellular components. In addition, nanofibres can be produced from materials which are biocompatible and biodegradable, such as polycaprolactone (PCL; 15), poly(lactic-*co*-glycolic acid) (PLGA) (15) and chitosan (16). Moreover, high surface area to volume ratio of nanofibres allows for good adsorption and high immobilization of cells as well as blood derivatives such as PRP (17).

Correspondence: R. Jakubova, Institute of Biophysics, 2nd Faculty of Medicine, Charles University in Prague, V Uvalu 84, 150 06, Prague 5-Motol, Czech Republic; and Laboratory of Tissue Engineering, Institute of Experimental Medicine, Academy of Sciences of the Czech Republic, v. v. i., Videnska 1083, Prague, Czech Republic. Tel./Fax: +420 296 442 387; E-mail: jakubova@biomed.cas.cz

The objective of this study was to establish functionalized nanofibres as a potential system for immobilization of thrombocytes and release of growth factors. PCL nanofibres were employed and the effect of immobilized thrombocytes on proliferation of chondrocytes attached to PCL nanofibres, was evaluated *in vitro*.

Materials and methods

Fabrication of PCL nanofibres

PCL nanofibres were prepared using an electrospinning method (18) from PCL with a molecular weight (MW) of 40 000 (Wako Chemicals GmbH, Neuss, Germany). Electrospinning was performed using 10% PCL dissolved in chloroform:ethanol (ratio 9:1). A high-voltage source generated voltages of up to 50 kV and the polymer solution was connected to the high-voltage source. Electrospun nanofibres were deposited on the grounded collecting electrode. Nanofibres were stored in a desiccator until use.

Preparation of thrombocyte-rich solution

PRP was obtained from the Hematology Service of the General Teaching Hospital, Prague, Czech Republic. PRP (volume 400 ml, thrombocyte concentration 225×10^9) was centrifuged (2250 ***g***, 15 min), supernatant was discarded and resulting thrombocytes were washed in washing buffer (pH 6.5, 113 mM NaCl, 4.3 mM K_2HPO_4, 4.3 mM Na_2HPO_4, 24.4 mM NaH_2PO_4 and 5.5 mM glucose) as described by Baenziger (19). Thrombocyte washing was repeated three to four times. Contaminating leukocytes and erythrocytes were removed by further centrifugation (120 ***g***, 7 min). Thrombocytes were then resuspended in 40 ml of washing buffer and centrifuged at 120 ***g*** for 7 min to recover thrombocytes that sedimented in the first 120 ***g*** spin. Thrombocytes were pelleted by centrifugation (2000 ***g***, 15 min) and washed once and finally resuspended in buffer pH 7.5 (109 mM NaCl, 4.3 mM K_2HPO_4, 16 mM Na_2HPO_4, 8.3 mM NaH_2PO_4 and 5.5 mM glucose). Manipulation of thrombocytes and thrombocyte-rich solution (TRS) was carried out in a sterile tissue culture hood in a clean room. TRS was stored in centrifuge tubes in a clean room until use. Temperature in the clean room was set at 22 °C.

Scaffold composite preparation

Before cell seeding, PCL nanofibres were cut into round patches of 6 mm diameter. Scaffolds were sterilized by immersing in 70% ethanol for 30 min and then washed three times in PBS (pH 7.4). PCL nanofibres were immersed in a thrombocyte-rich solution (380×10^6 thrombocytes/ml) for either 14 h (PCL14) or 2 h (PCL2), to enable adhesion. After the incubation time, such functionalized scaffolds were rinsed in PBS (pH 7.4), twice. The composite scaffold was placed into a new well and seeded with 9×10^4 chondrocytes/cm^2.

Cryo-field emission scanning microscopy

Cryo-field emission scanning microscopy (CryoSEM or FESEM) was performed for visualization of thrombocytes, as described previously (20,21). Briefly, samples were rapidly frozen in liquid nitrogen (−210 °C), then transferred to the cryo-stage of a preparation chamber (ALTO2500); there it was freeze-fractured at −140 °C, freeze-etched by raising sample temperature until sublimation of water began at −95 °C for 10 min, and then coated at −135 °C for 60 s with gold. After this, samples were placed on a cold-stage microscope and examined in the frozen state at −135 °C under suitably high voltage (1 kV using GB-H mode and 3 kV using GB-L mode) using a Jeol 7401-FE microscope.

Isolation and culture of chondrocytes

Chondrocytes were isolated and cultured as described previously, with slight modifications (22). Briefly, thin slices of articular cartilage were aseptically removed from the left femoral trochlea of mature pigs (Slaughter House; Cesky Brod, Czech Republic) within 2 h of killing. The cartilage was then cut into small pieces (~1 × 1 mm), placed into collagenase solution (0.9 mg/ml, collagenase NJB, SERVA) and incubated in a humidified incubator (37 °C, 5% CO_2) for 14 h. Cells were then centrifuged at 300 ***g*** for 5 min and seeded in culture flasks. The chondrocytes were then cultured in Iscove's modified Dulbecco's medium supplemented with 10% foetal bovine serum, penicillin/streptomycin (100 IU/ml and 100 μg/ml), 400 mM L-glutamine, 100 nM dexamethasone, 40 μg/ml ascorbic acid-2-phosphate and ITS – X (10 μg/ml insulin, 5.5 mg/l transferrin, 6.7 μg/l sodium selenite, 2 mg/l ethanolamine) at 37 °C in a humidified atmosphere with 5% CO_2.

Cell seeding

When cells became confluent, they were suspended using trypsin–EDTA; number of cells was determined using light microscopy. Chondrocytes were seeded on the scaffolds and TCP (tissue culture plastic) at 9×10^4/cm^2 cell density.

Cell proliferation analysis by MTT testing

A 50 μl solution of 3-(4,5-dimethylthiazol-2-yl)-2,5-diphenyltetrazolium bromide (MTT) (0.241 mmol) at 1 mg/ml concentration in phosphate-buffered saline (PBS), pH 7.4, was added to 150 μl of sample medium, and incubated for 4 h at 37 °C. The MTT component was reduced by mitochondrial dehydrogenase of metabolizing cells, to purple formazan. Formazan crystals were solubilized with 100 μl of 50% *N,N*-dimethylformamide in 20% sodium dodecyl sulphate at pH 4.7. Results were read at 570 nm wavelength (reference wavelength 690 nm), using an ELISA reader.

Confocal microscopy

To visualize the thrombocytes, staining for actin and P-selectin were performed. They were incubated in 4% paraformaldehyde solution (pH 7.2) in TBS (50 mM Tris–HCl, 150 mM NaCl, pH 7.4) for 20 min at 4 °C, then washed twice in TBS (pH 7.4). To permeabilize and block non-specific binding, the thrombocyte solution was incubated with 5% BSA and 0.5% Triton X-100 for 1 h at room temperature and washed twice again in TBS (pH 7.4). Phalloidin (phalloidin–tetramethylrhodamine B isothiocyanate; Sigma-Aldrich, Munich, Germany) and anti-P-selectin (CD62P antibody (C2) (FITC); Abcam, Cambridge, MA, USA) were added to the thrombocyte-rich solution and incubated overnight at 4 °C. Phalloidin–tetramethylrhodamine B isocyanate (1:50) and anti-P-selectin–FITC (1:500) in 1% BSA and 0.05% Triton X-100 solution were used to visualize the proteins. After washing twice in TBS, thrombocytes were resuspended in TBS (pH 7.4) solution (5 ml) before being observed using a Zeiss LSM 5 DUO confocal microscope (phalloidin–tetramethylrhodamine B isothiocyanate λ_{exc} = 540–545 nm and λ_{em} = 570–573 nm, anti-P-selectin-FITC λ_{exc} = 494 nm and λ_{em} = 518 nm).

To detect cell viability, live/dead cell staining (BCECF-AM/propidium iodide) was performed. Cells were stained with propidium iodide/BCECF- AM [2′,7′-bis (2carboxyethyl)-5(6)-carboxyfluorescein acetoxymethyl ester 1 mg/ml in dimethyl sulphoxide (DMSO) ≥ 95% HPLC] for detection of viability, and subsequently rinsed in PBS (pH 7.4). BCECF-AM (diluted 1:100 in medium) was then added to the scaffolds and incubated for 45 min at 37 °C and 5% CO_2; they were then rinsed in PBS (pH 7.4). Propidium iodide (5 μg/ml in PBS, pH 7.4) was added and allowed to stand for 10 min, rinsed in PBS (pH 7.4) again and visualized using the confocal microscope (BCECF-AM λ_{exc} = 488 nm and λ_{em} = 505–535 nm, propidium iodide λ_{exc} = 543 nm and λ_{em} = 630–700 nm). BCECF-AM is an intracellular fluorescent pH indicator, which is hydrolysed to BCECF by cytosolic esterases. Thus, only live cells contribute to staining results. Propidium iodide binds to double-stranded DNA, but it can only cross plasma membranes of non-viable cells. For each scaffold, number of live/dead cells was counted (software Ellipse) and averaged. Viability was calculated as percentage of live cells from total cell count per unit area. As control, thrombocyte-coated scaffold without chondrocyte seeding was scanned.

DiOC6 (3,3′-diethyloxacarbocyanine iodide) was used to detect adhesion of cells to scaffolds. Samples were fixed in frozen methyl alcohol (−20 °C) for 10 min, rinsed in PBS followed by DiOC6 (0.1–1 μg/ml in PBS; pH 7.4). After 45 min incubation at room temperature, samples were rinsed in PBS (pH 7.4), and propidium iodide (5 μg/ml in PBS; pH 7.4) was added and allowed to stand for 10 min, before being rinsed in PBS (pH 7.4) again and visualized using the confocal microscope (λ_{exc} = 484 nm and λ_{em} = 482–497 nm). Areas of adherent cells were determined (software Ellipse).

Cell adhesion

To measure cell adhesion, samples were fixed in methanol (−20 °C) for 10 min, rinsed in PBS (pH 7.4) and incubated in DiOC6 for 45 min. Stained cells were visualized using the Leica SP2 AOBS confocal microscope, and areas of attached chondrocytes were determined using the Ellipse software. For each scaffold, areas containing 100 cells were measured and averaged. Cell adhesion was also measured using the MTT assay as described above.

Quantitative real-time PCR analysis

Total RNA was extracted using an RNAeasy Mini Kit (Qiagen, Prague, Czech Republic) according to the manufacturer's protocol and were then stored at −20 °C. Synthesis of cDNA was performed by standard procedures as described previously (23). cDNA from 1 μg of RNA was used as template. Aggrecan mRNA expression levels were quantified by means of a light cycler 480 (Roche Diagnostic, Mannheim, Germany) using double-stranded-specific dye SYBR Green I (Roche Diagnostic) according to the manufacturer's instructions. Primers (Biogen, Prague, Czech Republic) used were as follows: aggrecan, sense 5′-ATGACAGAAAGCGACAAGGA-3′, antisense 5′-AAGCAGCAGTCACACCTGAG-3′; and beta-actin, sense 5′-ACAAAACCTAACTTGCGCAG-3′ and antisense 5′-TCCTGTAACAACGCATCTCA-3′. Samples were analysed in duplicate in a 96-well plate with final volume of 20 μl. Expression level of aggrecan mRNAs was adjusted using level of beta-actin mRNA as housekeeping level, and expressed as ratio to beta-actin. Evaluation of mRNA

expression of aggrecan was performed by quantitative real-time PCR analysis ($P < 0.05$, two-sided *t*-test).

Statistics

Quantitative data are presented as mean ± SD. For *in vitro* tests, average values were determined from four independently prepared samples. If not mentioned otherwise, results were evaluated statistically using one-way analysis of variance (ANOVA) and the Student–Newman–Keuls Method.

Results

Adhesion of PRP on PCL nanofibres

PCL nanofibres prepared by the electrospinning method with final surface mass of 0.18 g/m^2, were functionalized by adhering thrombocytes to them. Each small piece (0.33 cm^2) of PCL nanofibre mesh had been placed at the bottom of a 96-well plate and incubated with thrombocyte-rich solution (Fig. 1) at concentration of 380×10^6 thrombocytes/ml. To achieve thrombocyte immobilization, nanofibre scaffolds were pre-incubated with TRS for 2 h (PCL2 sample) and 14 h (PCL14 sample).

To demonstrate interaction between thrombocytes and PCL nanofibre mesh, cryo-field emission scanning microscopy (FESEM) was used and interactions were directly visualized; thrombocytes were found well adhered to PCL scaffolds (Fig. 2). Adhesion of thrombocytes to nanofibres was significant after as little as 2 h incubation and did not increase significantly in samples incubated for 14 h. Thus, 2 h pre-incubation of scaffolds with thrombocytes resulted in their effective immobilization on the nanofibre scaffold surface. We assume that increased adhesion is a result of directed cell migration towards thrombocytes and/or increased cell accommodation.

TRS visualization was achieved by confocal microscopy (Fig. 1). Thrombocytes were stained for actin and P-selectin expression as described in the Materials and methods section. P-selectin is expressed in alpha-granules of platelets and granules of endothelial cells and this platelet marker has been previously used for thrombocyte visualization (24). As a major dynamic protein, actin is highly abundant in platelets. Staining of these two markers provides evidence for presence of thrombocytes (Fig. 1).

Loss of activity of thrombocyte-rich solution

To employ immobilized thrombocytes as a potential nanoscale delivery system of native proliferation and differentiation factors, establishment of time-dependent degradation behaviour of thrombocytes in a physiological solution was necessary. Thus, effects of thrombocyte aging on chondrocyte proliferation were determined. Concentrated thrombocytes from PRP were either directly immobilized on scaffolds, which were subsequently seeded with chondrocytes, or thrombocyte-rich solution was stored at 22 °C. Aged TRS was applied after 3, 6, 8 and 16 days of storage, on the PCL nanofibre mesh. Subsequently, scaffolds were seeded with freshly prepared chondrocytes – similar to the case of newly prepared thrombocytes. Degradation of thrombocytes and loss of growth factor activity in solution, were assessed by absorbance values of MTT assay 7 days after cell seeding (day 7). Ability of aged thrombocytes to enhance chondrocyte proliferation gradually decreased (Fig. 3). Nevertheless, this loss of activity of thrombocyte releasate was relatively slow. TRS stored at 22 °C for a period shorter than 6 days still maintained ability to enhance chondrocyte proliferation. However, in cases of longer storage, degradation products of thrombocytes showed inhibitory effects and resulted in decrease of chondrocyte proliferation (Fig. 3).

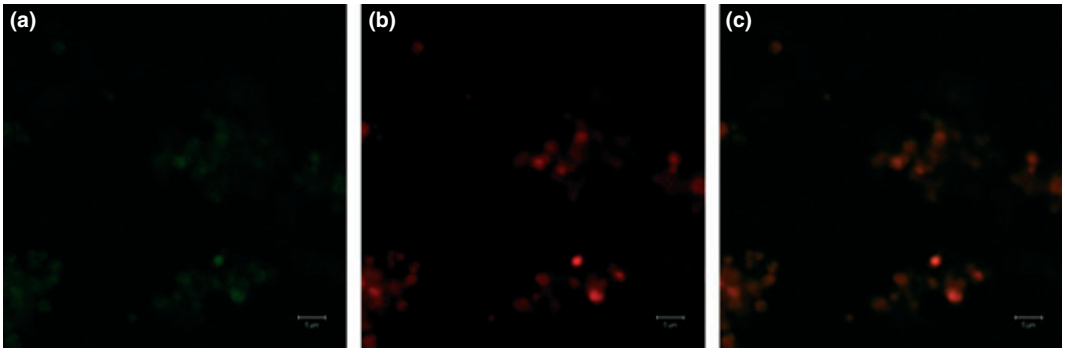

Figure 1. Thrombocyte visualization. Confocal microscopy of thrombocytes detected by anti-P-selectin immunostaining, with FITC, green (a) and anti-CD62 antibody, with tetramethylrhodamine B isocyanate (b), red. Part (c) represents superposition of (a) and (b), which resulted in orange (less intensive red) tint due to high actin/P-selectin signal ratio.

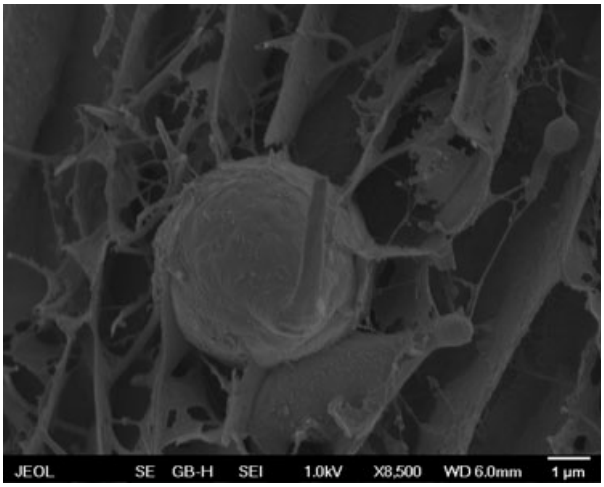

Figure 2. Thrombocyte visualization on nanofibres. CryoSEM visualization of thrombocytes on PCL nanofibres. Items seen in this figure have similar size and shape as thrombocytes, oval to round with diameters of 2–3 µm. Thickness of golden sputter coat used for visualization slightly increased their observed dimensions.

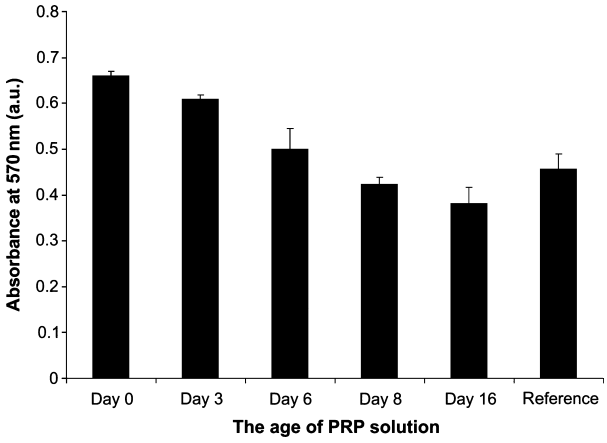

Figure 3. Degradation of thrombocyte-rich solution based on absorbance values of MTT assay. Nanofibre scaffolds pre-incubated for 2 h with aged TRS (stored at 22 °C for respective number of days – 0, 3, 6, 8, 16 as seen in graph visualizations) and subsequently seeded with freshly prepared chondrocytes. MTT assay was performed on day 7. TRS aging decreased proliferation with degradation half-life of approximately 3 days. Chondrocytes seeded on PCL scaffolds without thrombocytes were set as reference (refers to PCL sample in graph). Error bars refer to SD. Results compile measuring of four independent cell cultures per sample.

Adhesion of chondrocytes on PCL nanofibres with immobilized thrombocytes

Our experiment using freshly prepared TRS clearly showed its ability to enhance chondrocyte proliferation. However, chondrocyte population growth may be inhibited when incubated with aged TRS. This reflects complex related effects thrombocytes have on cell adhesion and proliferation, most likely due to high concentration of different growth factors they contain. In addition, while suitable thrombocyte concentration for cell proliferation in solution is easily controlled, administration of them to nanofibre scaffolds is difficult. Naturally, any nanofibre mesh is a quasi-2D system with unknown parameters significantly differing from natural 3D systems. Consequently, an empirical approach was necessary during this phase of our study.

To better understand effects of thrombocytes and the releasate, chondrocyte adhesion on the functionalized scaffolds (PCL nanofibres pre-incubated with TRS) was investigated. Such cell adhesion was compared to adhesion to the PCL scaffolds without addition of thrombocytes when cell seeded. In the latter case, scaffolds were not pre-incubated with TRS, but TRS was added to media after cell seeding. Cell visualization was achieved by confocal microscopy on day 1 (Fig. 4). Chondrocytes were stained with fluorescent dye (DiOC6) and propidium iodide as described in the Materials and methods section. DiOC6 is a lipophilic fluorescent stain for labelling membranes and other hydrophobic structures. Once applied to cells, the dye diffuses laterally within the plasma membranes, resulting in even staining of entire cell surfaces. Propidium iodide binds to double-stranded DNA of non-viable cells. It allows for accurate visualization of single cells.

Areas of attached chondrocytes (100 cells) were determined and cell adhesion was estimated. Increased chondrocyte adhesion on PCL nanofibres coated with thrombocytes was documented (Fig. 5). Cells seeded on functionalized nanofibres were significantly more spread out than those on nanofibres without thrombocytes. Interestingly, chondrocyte adhesion was greater on PCL14 samples than on PCL2 samples.

In addition, MTT assays were also performed on the first day after seeding, assuming that cell proliferation on day 1 was dependent on number of cells adherent to the nanofibres. To eliminate any contribution of non-adherent cells, each nanofibre sample was transferred to a new well on the plate for MTT assay. MTT test on day 1 showed an increased cell adhesion on nanofibres with thrombocytes compared to those on PCL alone (Fig. 6).

Proliferation of chondrocytes on PCL nanofibres with immobilized thrombocytes

More important than effects of thrombocytes on chondrocyte adhesion was their influence on cell proliferation. Chondrocyte proliferation on functionalized scaffolds was compared to proliferation on PCL scaffolds. Chondrocytes

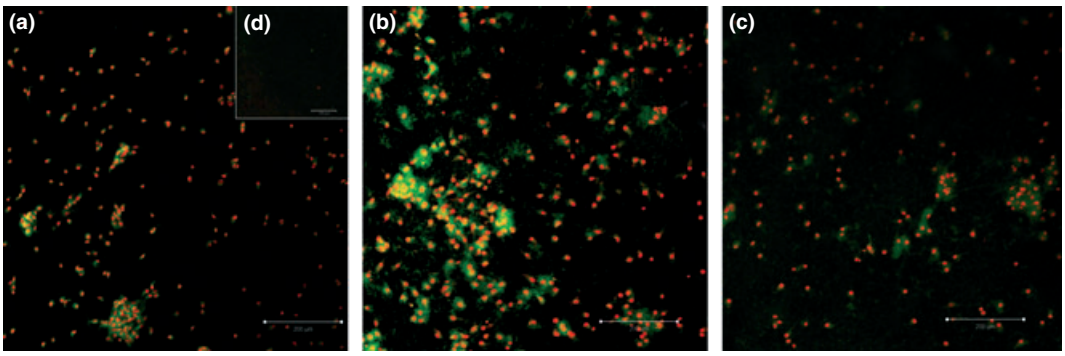

Figure 4. Adhesion of chondrocytes on PCL nanofibres; confocal microscopy. (a) PCL2; (b) PCL14; (c) PCL; (d) Control sample. Prior to chondrocyte seeding, PCL nanofibre scaffolds were pre-incubated with TRS for 2 h (PCL2) or 14 h (PCL14). PCL only represents non-treated scaffold (PCL). Non-seeded thrombocyte-coated scaffold served as control sample. Cell adhesion day 1 with (a) and (b) and without (c) immobilized thrombocytes. Most cells adhered on the PCL14 scaffold as seen (b). These cells spread out most over the same time frame. This image supports the hypothesis of ability of thrombocytes to stimulate cell migration and consequently cell adhesion to scaffolds.

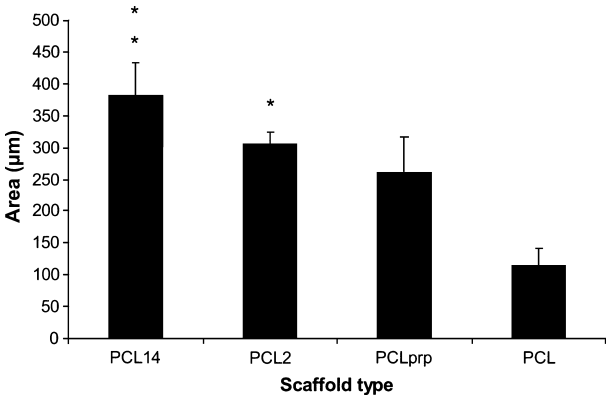

Figure 5. Chondrocyte adhesion on PCL nanofibres. Chondrocytes on functionalized matrix were stained with DiOC6 fluorescent dye to visualize living cells, as seen in Fig. 4. Cell areas were measured by confocal microscopy using Ellipsa software. Areas containing 100 cells were measured and averaged for each scaffold. PCL2 and PCL14 are samples with matrix coated by thrombocytes for the respective time. To PCLprp sample, thrombocytes were added to culture media after cell seeding. PCL sample represents control non-treated with thrombocytes. Error bars refer to SD. Significantly different values identified by asterisks (*$P < 0.01$; **$P < 0.05$) .

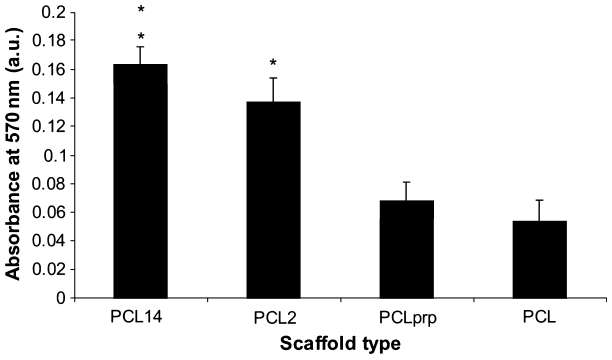

Figure 6. Adhesion of chondrocytes on PCL nanofibres; MTT assay. MTT assay performed on day 1. Each sample was transferred to a new well on the plate for MTT assay, thus, only adherent cells were involved. PCL2 and PCL14 – samples with matrix coated by thrombocytes. To PCLprp sample, thrombocytes were added to culture media after cell seeding. PCL sample represents control non-treated with thrombocytes. Error bars refer to SD. Significantly different values identified by asterisks (* $P < 0.01$; **$P < 0.05$).

on functionalized nanofibres showed a significant increase in proliferation on day 14 compared to those on PCL nanofibres only (Fig. 7). Interestingly, there was no significant difference in proliferation between cells on functionalized nanofibres and those on non-treated PCL scaffolds on day 7. This observation could be associated with a positive effect of PCL nanofibre scaffolds on chondrocyte proliferation. In combination with the fact that cell exposure to relatively high concentrations of proliferation and differentiation factors influenced biochemical pathways, a lag phase of cell proliferation resulted.

On day 14 however, proliferation of chondrocytes on PCL nanofibres alone decreased (Fig. 7), while chondrocyte proliferation on functionalized scaffolds was significantly higher. Notably, highest cell proliferation was observed on PCL2 samples.

A similar pattern was observed for cell viability. Cells were stained with propidium iodide/BCECF-AM and visualized by confocal microscopy. For each scaffold, number of live/dead cells was counted (software Ellipse) and averaged. Cell viability significantly increased on functionalized scaffolds on day 14 compared to non-coated scaffold. Highest viability was observed in samples that were pre-incubated for only 2 h with TRS (Table 1). However, no significant differences were observed on day

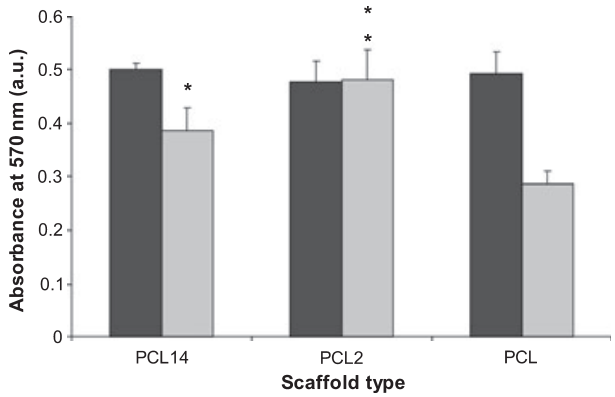

Figure 7. Chondrocyte proliferation on functionalized nanofibre scaffold. The MTT assay was performed on Day 7 (black bars) and Day 14 (hatched bars). Significantly different values with respect to the control PCL sample on the respective day are identified by asterisks (*$P < 0.01$; **$P < 0.05$). Error bars refer to SD.

Table 1. Chondrocyte viability on functionalized nanofibres

	% of cell viability on PCL14 samples	% of cell viability on PCL2 samples	% of cell viability on PCL samples
Day 7	87.4 ± 9.4	75.8 ± 1.4	77.1 ± 3.5
Day 14	76.6 ± 1.3	84.4 ± 1.1	54.8 ± 8.1

Percentage of chondrocyte viability on Day 7 and Day 14 based on propidium iodide/BCECF-AM staining and confocal microscopy. For each scaffold, the number of live/dead cells was counted (software Ellipse) and averaged. Table compiles results from four independent samples for each scaffold. Deviation in table represents SD.

7. Control samples, non-thrombocyte-coated scaffolds, were scanned; no contribution to background staining was observed.

Chondrocyte differentiation and real-time PCR results

Despite good chondrocyte proliferation on thrombocyte-coated scaffolds, whether or not cells were still able to maintain chondrocyte phenotype after culture in thrombocyte solution, remained unknown. To show chondrogenic phenotype of cells resulting from proliferation, relative expression level of aggrecan as a typical extracellular protein of cartilage, was determined using real-time PCR.

Maintenance of chondrocyte phenotype was confirmed for all tested samples 2 weeks after seeding. In accordance with our proliferation experiments, levels of aggregan mRNA on day 1 were significantly higher in samples not treated with thrombocytes (Fig. 8) compared to functionalized scaffolds. This most likely reflected the complex blend of differentiation and proliferation factors of thrombocytes. A completely different pattern, however,

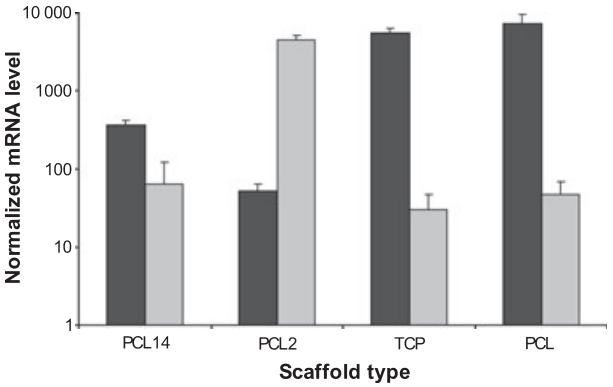

Figure 8. Aggrecan as a marker of chondrogenic expression. Aggrecan – chondrogenic marker expression, day 1 (black bars) and day 14 (striped bars), beta-actin used as housekeeping control. *Y*-axis, because of very different values, is a logarithmic scale. Evaluation of mRNA expression of aggrecan was performed by quantitative real-time PCR analysis ($P < 0.05$, two-sided *t*-test). Significantly different values with respect to control TCP sample is PCL2 on day 14. Error bars refer to SD. Graphic visualization of samples compiles results of four independent cell cultures.

was observed on day 14. Functionalized scaffolds preincubated in TRS for 2 h were found to best preserve chondrogenic phenotype of cells 2 weeks after seeding.

Discussion

Activity of thrombocyte-rich solutions

Cells of blood origin contribute to scar formation, accelerate skin wound repair and participate in healing processes (25,26). PRP as an essential derivative from blood platelets contains numerous growth factors, which can enhance cell proliferation (27). The regenerative potential of thrombocytes is based on release of growth factors that occurs when thrombocytes rupture. When autologous, their nature gives them a significant advantage and is pivotal for curing processes. Application of thrombocytes can also significantly affect and improve tissue engineering applications such as MSC proliferation and chondrogenic differentiation *in vitro* (28). Time-dependent decrease in number of circulation derivatives in a wounded area, similar to aging, destroys healing ability *in vivo* as well as cell proliferation *in vitro*.

We have shown in the framework of this study that thrombocyte aging influences its blend of natural growth factors. Ability of aged TRS to enhance chondrocyte proliferation slowly decreased when thrombocyte samples were stored at 22 °C. This slow decrease with half-life of approximately 2–3 days should be beneficial in possible clinical applications. Notably, in cases of longer storage, products of thrombocyte degradation showed inhibitory

effects and resulted in decrease of chondrocyte proliferation (Fig. 2). Lifespan of thrombocytes of approximately 7 days (29) has already been reported and correlates with our results.

Functionalized nanofibres as a nanoscale growth factor delivery system

Use of native autologous growth factors such as from thrombocytes, opens up new possibilities for tissue engineering to clinicians and researchers. To keep concentrations at bioactive levels for tissue repair or healing, a system for their immobilization must be developed.

The aim of this study was to overcome the major obstacle of thrombocyte delocalization and rapid removal. We have managed to immobilize thrombocytes on nanofibres and prepared functionalized nanofibre scaffolds with localized growth factors. These biocompatible and biodegradable PCL nanofibres efficiently immobilized thrombocytes after only 2 h pre-incubation in thrombocyte solution. Thrombocytes were not removed by rinsing in buffer. Locally higher concentration of natural growth factors appropriate for cells can create promising functionalized scaffolds in a useful drug delivery system.

Thrombocyte-functionalized PCL nanofibres enhanced chondrocyte proliferation

We found a proliferative effect of thrombocytes on chondrocytes and MSCs. This observation was in accordance with previous reports (30). However, our immobilized thrombocytes on nanofibres also worked successfully as a nanoscale delivery system of native proliferation and differentiation factors, improving both adhesion and proliferation of chondrocytes in our experiments *in vitro*.

Interestingly, there was no significant difference in chondrocyte proliferation between nanofibres coated with thrombocytes and non-coated PCL scaffolds 7 days after seeding, also indicated by aggrecan expression of PCL nanofibres. This was a typical consequence of growth factor depletion and higher concentrations of end-products (31). Such an observation can be associated with cell exposure to relatively high concentration of proliferation and differentiation factors influencing biochemical pathways, which results in a lag phase in cell proliferation. A completely different pattern on day 14 clearly proved a positive influence of thrombocyte-functionalized scaffolds on chondrocyte proliferation.

Time of coating with thromboyctes can also influence cell phenotype. This was reflected by elevated concentrations of aggrecan in samples PCL2 compared to PCL 14 and control samples (PCL, TPC), 2 weeks after seeding (Fig. 8).

Clearly, cultured cells are highly sensitive to medium composition. Two-hour pre-incubation of PCL nanofibres with TRS was found to be optimal for chondrocyte proliferation. We can hypothesize that longer pre-incubation times resulted in less favourable composition of growth factors for chondrocyte proliferation. Longer pre-incubation with thrombocytes, however, could be more favourable for proliferation of other cell types.

Seemingly, the role of PRP, thrombocytes and TRS in tissue engineering is quickly growing (32). Serum-free medium without addition of growth factors cannot cause cell numbers to expand *in vitro*. Thus, current research interests are focused on testing of different types of serum (foetal calf serum, autologous or allogeneic human serum) and PRP. Optimization of cell culture conditions, particularly for MSCs, to avoid interference with their self-renewal and differentiation processes and to assure durable engraftment and long-term therapeutic effects, evidently is crucial. Functionalized nanofibres with immobilized thrombocytes can undoubtedly contribute to this optimization.

Acknowledgements

This study was supported by the Academy of Sciences of the Czech Republic (Institutional research plans AV0Z50390703 and AV0Z50390512), Ministry of Education, Youth and Sports of the Czech Republic (research programs NPV II 2B06130, 1M0510, P304/10/1307), and Grant Agency of the Academy of Sciences grant no. IAA500390702 and by Czech Science Foundation grant no. GA202/09/1151, EU project BIOSCENT ID number 7E09088, the Grant Agency of the Charles University grants No.119009, 96610, 119209, 97110, 80009.

References

1 Sampson S, Gerhardt M, Mandelbaum B (2008) Platelet rich plasma injection grafts for musculoskeletal injuries: a review. *Curr. Rev. Musculoskelet. Med.* **1**, 165–174.
2 Alsousou J, Thompson M, Hulley P, Noble A, Willett K (2009) The biology of platelet-rich plasma and its application in trauma and orthopaedic surgery: a review of the literature. *J. Bone Joint Surg. Br.* **91**, 987–996.
3 Hall MP, Band PA, Meislin RJ, Jazrawi LM, Cardone DA (2009) Platelet-rich plasma: current concepts and application in sports medicine. *J. Am. Acad. Orthop. Surg.* **17**, 602–608.
4 Kuznetsov SA, Mankani MH, Gronthos S, Satomura K, Bianco P, Robey PG (2001) Circulating skeletal stem cells. *J. Cell Biol.* **153**, 1133–1140.
5 Kajikawa Y, Morihara T, Watanabe N, Sakamoto H, Matsuda K, Kobayashi M *et al.* (2007) GFP chimeric models exhibited a biphasic pattern of mesenchymal cell invasion in tendon healing. *J. Cell. Physiol.* **210**, 684–691.
6 Volkman A, Gowans JL (1965) The production of macrophages in the rat. *Br. J. Exp. Pathol.* **46**, 50–61.

7 Ma Z, Kotaki M, Inai R, Ramakrishna S (2005) Potential of nanofiber matrix as tissue-engineering scaffolds. *Tissue Eng.* **11**, 101–109.

8 Roldan JC, Jepsen S, Miller J, Freitag S, Rueger DC, Açil Y *et al.* (2004) Bone formation in the presence of platelet-rich plasma vs. bone morphogenetic protein-7. *Bone* **34**, 80–90.

9 Lucarelli E, Fini M, Beccheroni A, Giavaresi G, Di Bella C, Aldini NN *et al.* (2005) Stromal stem cells and platelet-rich plasma improve bone allograft integration. *Clin. Orthop. Relat. Res.* **435**, 62–68.

10 Akeda K, An HS, Okuma M, Attawia M, Miyamoto K, Thonar EJ *et al.* (2006) Platelet-rich plasma stimulates porcine articular chondrocyte proliferation and matrix biosynthesis. *Osteoarthritis Cartilage* **14**, 1272–1280.

11 Nagae M, Ikeda T, Mikami Y, Hase H, Ozawa H, Matsuda K *et al.* (2007) Intervertebral disc regeneration using platelet-rich plasma and biodegradable gelatin hydrogel microspheres. *Tissue Eng.* **13**, 147–158.

12 Anitua E, Sanchez M, Orivea G, Andia I (2007) The potential impact of the preparation rich in growth factors (PRGF) in different medical fields. *Biomaterials* **28**, 4551–4560.

13 Sanchez AR, Sheridan PJ, Kupp LI (2003) Is platelet-rich plasma the perfect enhancement factor? A current review. *Int. J. Oral Maxillofac. Implants* **18**, 93–103.

14 Everts PA, Brown Mahoney C, Hoffmann JJ, Schönberger JP, Box HA, van Zundert A *et al.* (2006) Platelet-rich plasma preparation using three devices: implications for platelet activation and platelet growth factor release. *Growth Factors* **24**, 165–171.

15 Kim TG, Park TG (2006) Surface functionalized electrospun biodegradable nanofibers for immobilization of bioactive molecules. *Biotechnol. Prog.* **22**, 1108–1113.

16 Jayakumar R, Prabaharan M, Nair SV, Tamura H (2010) Novel chitin and chitosan nanofibers in biomedical applications. *Biotechnol. Adv.* **28**, 142–150.

17 Hromadka M, Collins JB, Reed CH, Li K, Kamal K, Bruce A *et al.* (2008) Nanofiber applications for burn care. *J. Burn Care Res.* **29**, 695–703.

18 Lukas D, Sarkar A, Martinova L, Vodsedalkova K, Lubasova D, Chaloupek J *et al.* (2009) Physical principles of electrospinning (electrospinning as a nano-scale technology of the twenty-first century). *Textile Progress* **41**, 1–83.

19 Baenziger NL, Brodie GN, Majerus PW (1971) A thrombin-sensitive protein of human platelet membranes. *Proc. Natl. Acad. Sci. USA* **68**, 240–243.

20 Ruzek D, Vancova M, Tesarova M, Ahantarig A, Kopecky J, Grubhoffer L (2009) Morphological changes in human neural cells following tick-borne encephalitis virus infection. *J. Gen. Virol.* **90**, 1649–1658.

21 Erlandsen SL, Ottenwaelter C, Fretham C, Chen Y (2001) Cryo field emission scanning electron microscopy. *Biotechniques* **31**, 300–305.

22 Filova E, Rampichova M, Handl M, Lytvynets A, Halouzka R, Usvald D *et al.* (2007) Composite hyaluronate-type I collagen-fibrin scaffold in the therapy of osteochondral defects in miniature pigs. *Physiol. Res.* **56**, 5–16.

23 Tvrdik D, Svatošová J, Dundr P, Povýšil C (2005) Molecular diagnosis of synovial sarcoma: detection of SYT-SSX11/2 fusion transcripts by RT-PCR in paraffin-embedded tissue. *Med. Sci. Monit.* **11**, MT1–MT7.

24 Yang H, Lang S, Zhai Z, Li L, Kahr WHA, Chen P *et al.* (2009) Fibrinogen is required for maintenance of platelet intracellular and cell-surface P-selectin expression. *Blood* **114**, 425–436.

25 Bucala R, Spiegel LA, Chesney J, Hogan M, Cerami A (1994) Circulating fibrocytes define a new leukocyte subpopulation that mediates tissue repair. *Mol. Med.* **1**, 71–81.

26 Chesney J, Bucala R (1997) Peripheral blood fibrocytes: novel fibroblast-like cells that present antigen and mediate tissue repair. *Biochem. Soc. Trans.* **25**, 520–524.

27 Freymiller EG, Aghaloo TL (2004) Platelet-rich plasma: ready or not? *J. Oral Maxillofac. Surg.* **62**, 484–488.

28 Mishra A, Tummala P, King A, Lee B, Kraus M, Tse V *et al.* (2009) Buffered platelet-rich plasma enhances mesenchymal stem cell proliferation and chondrogenic differentiation. *Tissue Eng. Part C Methods* **15**, 431–435.

29 Dumont LJ, VandenBroeke T (2003) Seven-day storage of apheresis platelets: report of an in vitro study. *Transfusion* **43**, 143–150.

30 Drengk A, Zapf A, Stürmer EK, Stürmer KM, Frosch KH (2009) Influence of platelet-rich plasma on chondrogenic differentiation and proliferation of chondrocytes and mesenchymal stem cells. *Cells Tissues Organs* **189**, 317–326.

31 Heywood HK, Lee DA (2008) Monolayer expansion induces an oxidative metabolism and ROS in chondrocytes. *Biochem. Biophys. Res. Commun.* **373**, 224–229.

32 Tonti GA, Mannello F (2008) From bone marrow to therapeutic applications: different behaviour and genetic/epigenetic stability during mesenchymal stem cell expansion in autologous and foetal bovine sera? *Int. J. Dev. Biol.* **52**, 1023–1032.